Results of the Compensated Earth–Moon–Earth Retroreflector Laser Link (CEMERLL) Experiment

K. E. Wilson
Communications Systems and Research Section

P. R. Leatherman, R. Cleis, J. Spinhirne, and R. Q. Fugate
Air Force Laboratory, Kirtland Air Force Base, New Mexico

Adaptive optics techniques can be used to realize a robust low bit-error-rate link by mitigating the atmosphere-induced signal fades in optical communications links between ground-based transmitters and deep-space probes. Phase I of the Compensated Earth–Moon–Earth Retroreflector Laser Link (CEMERLL) experiment demonstrated the first propagation of an atmosphere-compensated laser beam to the lunar retroreflectors. A 1.06-μm Nd:YAG laser beam was propagated through the full aperture of the 1.5-m telescope at the Starfire Optical Range (SOR), Kirtland Air Force Base, New Mexico, to the Apollo 15 retroreflector array at Hadley Rille. Laser guide-star adaptive optics were used to compensate turbulence-induced aberrations across the transmitter's 1.5-m aperture. A 3.5-m telescope, also located at the SOR, was used as a receiver for detecting the return signals. JPL-supplied Chebyshev polynomials of the retroreflector locations were used to develop tracking algorithms for the telescopes. At times we observed in excess of 100 photons returned from a single pulse when the outgoing beam from the 1.5-m telescope was corrected by the adaptive optics system. No returns were detected when the outgoing beam was uncompensated. The experiment was conducted from March through September 1994, during the first or last quarter of the Moon.

I. Introduction

Optical communications technology is fast evolving in both the NASA and Department of Defense (DOD) communities as a viable telecommunications option between Earth-based stations and near-Earth satellites and deep-space probes. As demands grow for smaller spacecraft to return larger volumes of data, the lower mass, smaller size, and high-data-rate advantages of optical communications subsystems make this technology attractive to mission designers [1]. The technology has fast begun to gain greater acceptance after researchers demonstrated its viability in low-cost space-to-ground demonstrations to a geostationary satellite [2] and in the ground-to-space link to the Galileo spacecraft in deep space [3,4].

Devising low-cost strategies to mitigate the effects of the atmosphere on laser-beam propagation has been a key impediment to the acceptance of free-space optical communications. Cloud cover, atmospheric-turbulence-induced scintillation, and beam wander can cause deep fades in the uplink beam power and

degrade the optical channel. Optical communications demonstrations [5–7] have explored strategies to mitigate these effects. Cloud cover effects can be reduced by placing the ground station in locations of uncorrelated or anticorrelated weather patterns [8]. Such site diversity of ground stations is becoming more economically attractive as the costs of the 1-m class telescopes to support low Earth-orbiting (LEO) missions continue to decline.[1]

For LEO and geostationary (GEO) links, uplink signal fades induced by beam wander and scintillation are mitigated by using either multiple-beam uplinks [2] or adaptive optics. In the multiple-beam approach, spectrally incoherent laser beams are transmitted from apertures separated by greater than the Fried [9] atmospheric coherence cell size [r_o] so that they incoherently add at the receiver on the spacecraft. Theoretical predictions show that a multibeam approach that uses less than 5-W output power from ground-based lasers can provide adequate margin in a ground-to-LEO satellite optical link to compensate for atmospheric scintillation and beam wander. Theory also shows that these laser power levels would support reliable bidirectional communications of several hundred megabits per second [10]. However, as link ranges increase, the multibeam propagation using wide ($\sim$30 μrad) uplink beams to mitigate scintillation and beam wander may no longer be a viable approach. This is particularly true for communications with deep-space probes, where the need for high-quality kilowatt-class lasers is already approaching the state of the art.

For deep-space links where ranges are measured in astronomical units, telecommunications system designers will have to find ways of mitigating the atmospheric turbulence so that near-divergence-limited beams can be used to uplink commands to the spacecraft [11]. The divergence of an uncompensated laser beam uplinked through the atmosphere is limited by atmospheric seeing, and this can range from 2 to 20 μrad, depending on the time of day and location. Relative to diffraction-limited performance, atmospheric-seeing-limited divergence imposes a 6- to 10-dB power penalty on a 1-μm wavelength beam uplinked through a 1-m class telescope. At the uplink laser power levels currently baselined at 1 kW (4 J in a 10-ns-pulse 250-Hz repetition rate) for deep-space links, near-diffraction-limited beam divergence ($\sim$2 μrad) from 1-m class apertures can achieve the required optical uplink performance to a deep-space probe at Pluto. Such narrow-beam divergence requires the use of adaptive optics to compensate for atmospheric effects and allow near-diffraction-limited beam propagation through the atmosphere. Although monochromatic laser guide-star adaptive optics (LGAO) does not correct for wavefront tilt, it can correct higher-order atmosphere-induced aberrations and mitigate atmospheric scintillation that causes beam spreading. LGAO is the first step in achieving near-diffraction-limited beam propagation from 1-m class telescopes [12].

In this article, we report on the results of the first atmosphere-compensated laser beam propagation to the lunar retroreflectors. The Compensated Earth–Moon–Earth Retroreflector Laser Link (CEMERLL) experiment was jointly performed by the U.S. Air Force Phillips Laboratory's Starfire Optical Range (SOR) and the Jet Propulsion Laboratory. In Section II, we discuss the experiment and preparations for propagating the Nd: YAG beam. We describe the transmitter in Section III. The receiver system at the 3.5-m telescope is described in Section IV, and the calibration of the detector is given in Section V. Results are given in Section VI and conclusions in Section VII.

II. Experiment Description

The objectives of the CEMERLL demonstration were distinctly different from those of conventional laser lunar-ranging systems. This was reflected in the design of the detection system, where the focus was to measure the number of returned photons as opposed to accurately knowing their arrival times. The experiment was conducted at the Starfire Optical Range facility, Kirtland Air Force Base, New Mexico, from March through September 1994. A Q-switched Nd:YAG beam was compensated for atmospheric

[1] B. Greene, CEO, EOS Pty Ltd., and L. Randall, EOS, personal communication, January 17, 1997.

turbulence and transmitted from the 1.5-m telescope at the SOR to the Apollo 15 corner-cube array near Hadley Rille [13,14]. The location of the Apollo 15 lunar reflectors is shown in Fig. 1 along with the Russian Lunakhods and the Apollo 11 and Apollo 14 reflectors. The retroreflected laser pulse was collected at the 3.5-m telescope. The experiment was conducted during either the first or last quarter phases of the Moon when the retroreflectors were in the dark area of the lunar landscape. The objective of the experiment was to evaluate the benefits of adaptive optics to free-space laser communications [15] by comparing the statistics of uncompensated and compensated laser beam propagation [16,17]. Because the uplinked beam was retroreflected from corner cubes, the statistics of the returns reflect the statistics of the uplink beam propagation.

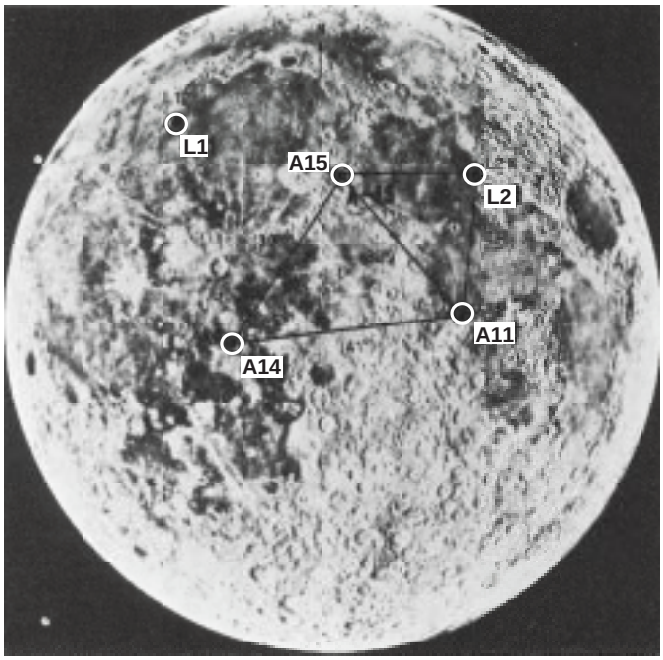

Fig. 1. Locations of Apollo and Lunakod reflector packages on the Moon [14].

To be useful in optical communications, the adaptive optics system must correct for both atmosphere-induced scintillation and beam spreading and for the low-order full-aperture tilt that causes beam jitter. For uplink transmission, these effects are best corrected by using an exo-atmospheric beacon that leads the target by a point-ahead angle, $2u/c$. The cross-velocity of the target relative to the transmitter is u, and c is the speed of light. Phase distortions accumulated by the beacon as it propagates down through the atmosphere are detected at the transmitter facility and used to predistort the uplink beam propagated through the same patch of atmosphere. Higher-order aberrations are corrected using a deformable mirror (i.e., a thin, flexible face sheet whose optical figure can be set by electrically controlled actuators pushing and pulling on its back surface). Lower-order aberrations are corrected using a two-axis fast steering mirror.

Using an exo-atmospheric guide star for CEMERLL would have required that a bright star be within the atmospheric isoplanatic patch [18] for the duration of the experiment. This requirement clearly could not be met, given the difference in the velocities of the stars and the Moon. In addition, the nominal 12-μrad isoplanatic angle at 1.06 μm is much less than the approximate 3-mrad angular distance between the edge of the moon and the Apollo 15 array. A natural guide star at this large angular separation would not have allowed compensation for atmospheric aberrations in an atmospheric path transited by the uplink beam. We therefore used a laser guide star created by the Rayleigh backscatter from a copper

vapor laser (CVL) to compensate for the higher-order aberrations caused by atmospheric turbulence. Tilt correction was not done in this phase of CEMERLL and was to be the focus of a Phase II experiment.

Under typical atmospheric conditions, the uncompensated 1.06-μm laser beam from the transmitter telescope is spread by the atmosphere to a $1/e^2$ full-width intensity of 17 μrad. This is decreased to less than 3 μrad when the laser beam is compensated using adaptive optics. To correct for atmospheric effects, a CVL was focused to create a guide star 10-km above the transmitting telescope. A detector array at the transmitter was gated to sample the light scattered back to the telescope from the guide star. The detector array was servoed around the deformable mirror; higher-order atmosphere-induced aberrations measured by the Shack–Hartman sensor were processed and fed back to the deformable mirror. The mirror then predistorted the outgoing laser beam so that the beam was nearly diffraction limited at the top of the atmosphere.

The lunar reflectors are not visible from Earth. To illuminate them, familiar lunar features had to be used as references to offset point the narrow laser beam to the target. To test the blind-pointing capability of the telescope, bright stars near the Moon were used as references to offset point to lunar features. The test results proved that both telescopes could blind point to better than the beam width of the compensated beam. Extended-source tracking was unavailable at the time of the experiment, and we used the JPL-supplied pointing vectors to track the retroreflectors as the Moon transited the sky. The pointing vectors were corrected for the 6- to 7-μrad lunar point-ahead angle. Transmission was interrupted periodically to verify that both transmitter and receiver telescopes remained pointed at the target.

III. The Transmitter

The transmitter telescope was a 1.5-m, 10X magnification, azimuth/elevation telescope made by Contraves. It was operated in a coudé feed configuration that coupled the telescope to the laser transmitter in a laboratory two stories below the pier. A detailed description of the optical arrangement of the 1.5-m telescope has been given previously [12] and will not be repeated here. We do discuss, however, the coudé path modification that was needed to propagate and to accurately point a high-power laser beam from the telescope.

While an intermediate focus in a telescope's coudé optical path may prove useful in certain applications, it can be problematic when propagating a high-powered laser beam. High-powered laser beams when focused in air generally result in an arc discharge that is caused either by air breakdown or by vaporization of dust particles in the beam path. In CEMERLL, arcing of the laser beam was caused by dust particles transiting the beam in the vicinity of the coudé intermediate focus. This initially prevented laser operation at the power levels needed to observe returns from the lunar retroreflectors. Two approaches to eliminate this problem and allow full-power operation were considered. These were (1) to blow dry nitrogen across the beam in the vicinity of the focus to keep dust out of the beam and (2) to install an evacuated tube with optical windows around the intermediate focus.

The flowing nitrogen approach was more complicated to implement. However, it did have the advantage of not introducing additional optical elements into the coudé path that could degrade the quality of the images used to guide the telescope. The beam tube approach was straightforward and was attempted first. Our concerns about introducing aberrations into the imaging path were allayed when tests of the high-quality optical flats to be used showed that phase distortions introduced by these windows were negligible. The first pair of windows was antireflection coated to reduce the 16 percent Fresnel losses at the four glass–air interfaces to less than 4 percent. However, the high laser power densities on the windows in the converging beam damaged the coatings. We replaced the windows with uncoated fused silica blanks, and these operated without damage for the duration of the experiment. We operated the laser at full power with the tube in place and propagated 340-mJ, 15-ns-wide laser pulses to the Moon.

IV. The Receiver

Laser pulses retroreflected from the lunar array were collected by the 3.5-m telescope that was located approximately 100-m west-northwest of the 1.5-m telescope. A relay optical train with detector was assembled on a small breadboard attached to the Nasmyth focus of the telescope. Theory predicted that the maximum expected compensated beam return was 15-dB greater than that of the uncompensated beam [17]. However, when weighted by the expected low frequency of returns for the tilt-uncorrected case, the predictions show that on average the expected return between the two beams would be comparable. Without tilt correction, the narrower compensated beam would jitter on and off the target and illuminate the retroreflectors less frequently than would the broader uncompensated beam. The predictions were 117 photons for an uncompensated beam and 205 photons for a nominal 2-μrad atmosphere-compensated beam.

Over the course of the experiment, two different detectors were used at the receiving facility. The first, an enhanced avalanche photodiode (APD), was used for experiments from March through July 1994. No returns were detected. Inclement weather precluded transmissions in March and May, and satellite predictive avoidance conflicts precluded all but 1 hour of transmission in June. When using the APD detectors for transmissions during April and June, the detectors became saturated from prolonged viewing of the background light from the dark side of the Moon. Attempts to reduce the background below saturation by using a 1-nm filter were unsuccessful. The detectors remained saturated for several hours after exposure.

The second detector, an experimental back-illuminated solid-state photomultiplier (SSPM) device built by the Rockwell Science Center, was first used on August 26, 1994, the first of the three propagation opportunities during the Moon's last quarter in August. The SSPM had a quantum efficiency of 6 to 8 percent at 1.06 μm and an active area of 800 $\times$ 800 μm that corresponded to a 70-μrad field of view at the f/5.6 Nasmyth focus. The detector was integrated with a high-speed transimpedance amplifier that had low- and high-sensitivity gain settings. The detector was enclosed in an Infrared Laboratories' liquid-helium-cooled dewar and located approximately 5-cm behind a 10-nm filter centered at 1064 nm. It was operated at 11 K with its temperature controlled using a Lakeshore model 805 temperature regulator. As was observed with the APD, the infrared signature from the dark side of the Moon as viewed through the 10-nm filter was large, and it would have masked any return signals. A 1-nm wide, 61 percent transmission interference filter was added in the optical train for further background suppression. With the two filters in place, we were able to detect the return signals.

V. Receiver Calibration

Because at the time of the experiment the SSPM was an experimental device still under study, detector calibration curves were not available from the manufacturer. The 10-nm filter came with the device in its dewar, and the integrated system was treated as a black box. We used a two-step approach to characterize and calibrate the unit. The first step was to use the Rayleigh backscatter from Nd:YAG laser pulses propagated vertically from the 1.5-m telescope to characterize the transfer function of the 3.5-m telescope. The second step was to measure the signal strength of well-known bright stars and compare the measurements with theory. Both measurements were made on the same night to ensure that the atmospheric conditions remained essentially unchanged during the test interval. The results are shown in Figs. 2 through 4 for the SSPM on the low-gain setting.

Results from the Rayleigh backscattered signal strength measured as a function of range from the receiver telescope are shown in Fig. 2. Also shown in the figure is the return signal predicted using a modified version of the light detection and ranging (LIDAR) equation [19, p. 239] given below:

$$P(r) = a_1 a_2 \eta P_t \frac{A}{r^2} \beta \frac{c\tau}{2} e^{[-2\int_0^r \sigma(x)dx]} \tag{1}$$

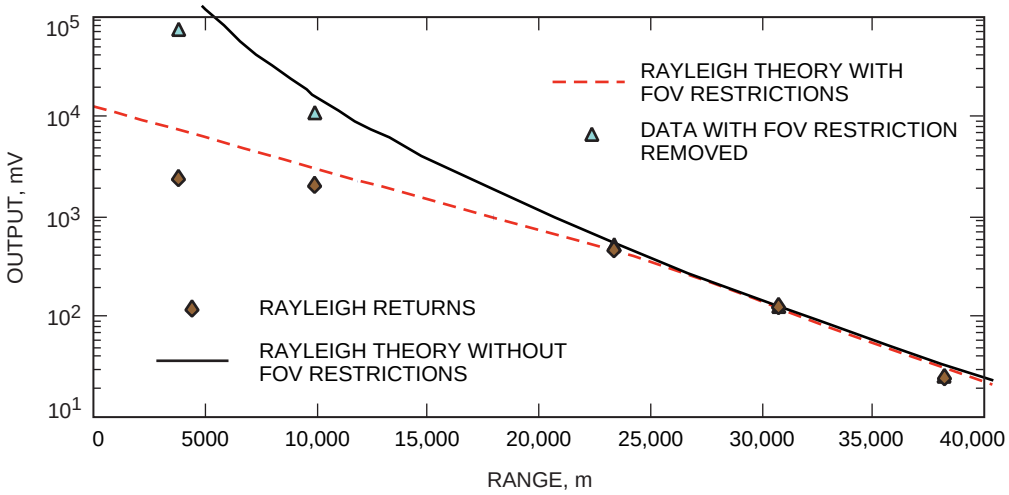

Fig. 2. SSPM output versus range data collected. Evidence of detector saturation is seen in the two largest returns at the lower ranges.

In Eq. (1), $P(r)$ is the received power from range r, and a_1 is the backscatter angle-correction factor (i.e., the correction for the angle between the beam propagation direction and the receiver telescope optical axis). The ratio of the receiver's field of view (fov) to the angular width of the transmitted beam is given by a_2. This has a maximum value of 1 when the entire transmitted beam lies within the receiver's fov. The transmitted laser power is P_t, the transmission efficiency of the optical train is η, and the speed of light is c. In Eq. (1), A is the area of the receiver, τ is the sampling interval, and σ is the attenuation coefficient; β is the backscatter coefficient given by [19, p. 42]

$$\beta = 1.39 \left[\frac{0.55}{\lambda(\mu m)} \right]^4 \times 10^{-6} m^{-1} sr^{-1} \tag{2}$$

With the SSPM at the focus, the fov of the 3.5-m telescope was limited to 70 μrad. Thus, at the lower ranges, the angle subtended by the 1.5-m transverse width of the backscattered beam exceeded the receiver's fov.

The Rayleigh backscatter data collected over three consecutive nights in August 1994 are given in Fig. 2. Each data point is an average of 144 Rayleigh backscatter returns. The solid line shown in the figure is the theoretical Rayleigh backscatter strength predicted by Eq. (1) without the fov limitation. The dashed line shows the theoretical backscatter as modified by the detector's field of view.

At ranges below 25 km, the uplink laser beam subtended an angle larger than the 70-μrad fov of the SSPM. The detector thus collected light from a portion of the outgoing laser's cross-section. The full beam power was used for the theoretical calculations of the backscattered signal strength for ranges greater than 25 km. The diamonds in Fig. 2 are the collected Rayleigh returns, while the triangles are the same returns scaled to compensate for the limited fov of the detector. The lower-than-predicted Rayleigh returns at ranges below 15 km are suspected to be due to detector saturation. This is shown in Fig. 2 by the leveling off of the return signal strength at these lower ranges.

Figure 3 gives the SSPM responsivity determined from the Rayleigh backscatter measurements shown in Fig. 2. Only those points below the saturation of the detector were used for Fig. 3. The figure shows the SSPM's responsivity at this low-gain setting to be 0.142 photons/mV.

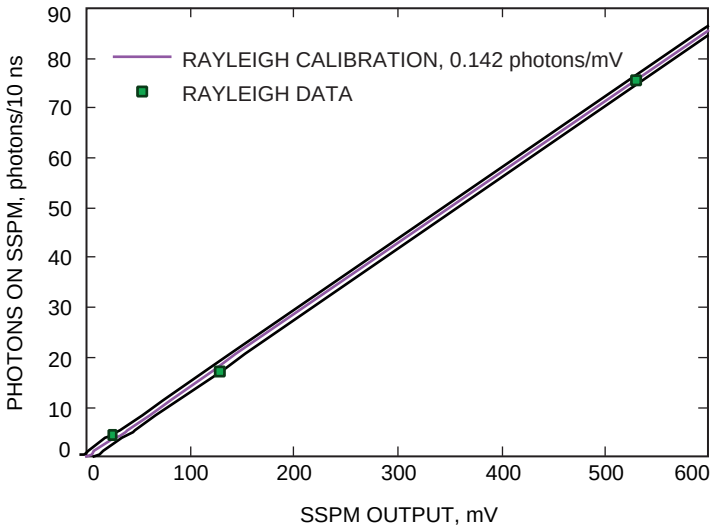

Fig. 3. The calibration of the SSPM using data from the Rayleigh backscatter from various ranges. The outer lines represent ±σ (one standard deviation for the fit of the data).

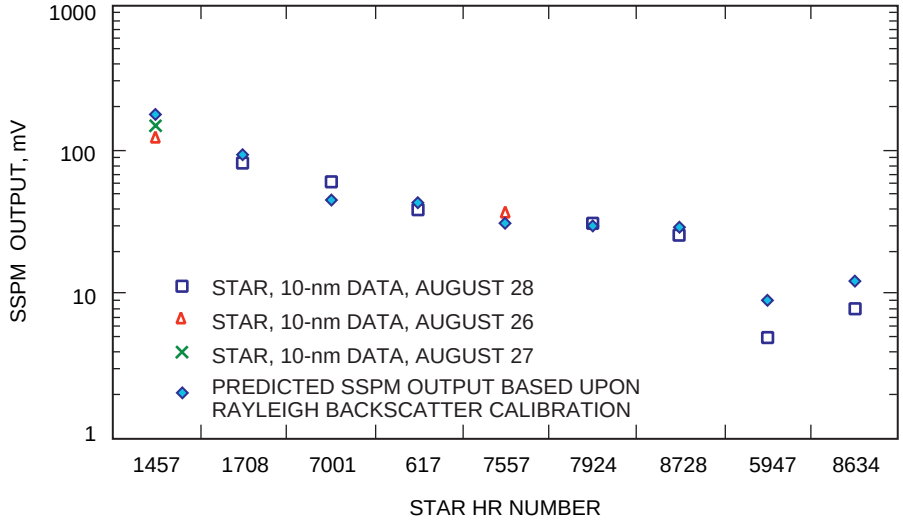

Fig. 4. Measurements from 9 bright stars made through the 10-nm filter. The transmission of the built-in 10-nm filter is included in the calculation. The predicted points were calculated using the detector responsivity (photons/10 nm/mV) determined from Rayleigh backscatter measurements made on the same nights.

Measurements from 9 bright stars made through the 10-nm filter are shown in Fig. 4. The selected stars either had well-known color indices or their spectral classes were well defined. The data, an average over 40 traces on a model 9414 LeCroy oscilloscope, are shown along with the expected signal return calculated using [20]

$$f_{\lambda_{top}} = c_1 10^{-0.4 m_v} \frac{\left(e^{c_2/0.55T_{eff}} - 1\right)}{\left(e^{c_2/\lambda T_{eff}} - 1\right)} \lambda^{-4} \tag{3}$$

Except for the dimmest stars, HR 5947 and HR 8634, measurement and theory given by Eq. (3) show good agreement.

In Eq. (3), $f_{\lambda_{top}}$ is the photon flux density at the top of the atmosphere, $c_1 = 9.627 \times 10^8$, and $c_2 = 1.44 \times 10^4$. The wavelength in microns is β, the star's effective temperature is T_{eff}, and the star's apparent visual magnitude is m_v. This equation was corrected for atmospheric transmission using the expression given in

$$f_{\lambda_{bot}} = f_{\lambda_{top}} e^{(-\zeta \text{ sec } z)} \tag{4}$$

In Eq. (4), ζ is given by [20]

$$\zeta = e^{(y_1 + y_2 - 5.6399)} \tag{5}$$

where y_1 and y_2 are wavelength-dependent variables given by

$$y_1 = 3.7886 e^{\left[\frac{-(\ln\lambda + 130605)^2}{0.02338}\right]} \tag{6}$$

and

$$y_2 = 26.911 e^{\left[\frac{-(\ln\lambda + 5.8466)^2}{14.236}\right]} \tag{7}$$

In Eq. (4), (sec z) is the secant of the zenith angle, i.e., the air mass of the star's location.

The theoretical results shown in Fig. 4 are a posteriori values, i.e., a priori values corrected for the receiver's transfer function obtained from Rayleigh backscatter data. The SSPM calibration constant obtained from a fit to the star data in Fig. 4 was 7.8 mV/photon. This is comparable to the 7 mV/photon (0.142 photons/mV) obtained from the Rayleigh measurements given in Fig. 3.

VI. Lunar Transmission Results

The round-trip light-time to the array is approximately 2.7 s, and this changes as the Moon transits the sky. The timing sequence for initiating a detection window began with a trigger signal generated by the outgoing Nd:YAG laser pulse at the 1.5-m telescope. Using the ephemeris predicts and the signal generated by the outgoing pulse, a computer calculated the expected arrival time of the return signal. A time interval counter kept track of the delay and at the appropriate time sent a trigger signal on a dedicated line to the scalar averager at the receiver facility to initiate the detection window. The trigger delay was adjusted to accommodate the finite transit time of the electronic signal between the two facilities. It also was continuously adjusted to correct for the changing round-trip light-time to the retroreflectors as the moon transited the sky.

Transmissions with the SSPM detector began on August 26 and proceeded through August 28. Lunar transmissions were preceded by a SSPM measurement of the intensity of star HR 617. This procedure allowed characterization of the atmospheric transmission and evaluation of the detector's performance from one day to the next. Over this 3-day period, inclement weather allowed only 2 hours of transmission, and no returns were observed. A review of our experimental arrangement did not reveal any omissions or flaws. Because of the difficulty in visually resolving signal returns from the background noise, we decided to add a scalar averager to our detection system for the September transmissions.

In September, the SSPM detector was integrated with a Stanford Research Systems SRS 430 scalar averager detection system that counted positive voltage transitions over a preset level. Returns were observed on September 27, 28, and 29, the three nights of transmissions to the lunar array. Transmissions scheduled for September 30 were canceled because of inclement weather. Twenty-five returns were

detected over the 3-day period. Several returns saturated the detector, indicating a return rate in excess of 100 photons incident on the dewar. On September 27, the SSPM was set on low gain, and four sets of returns were detected over a 45-min period before a power outage at the transmitter facility prevented further operation. On September 28, the detector was set on high gain, and over one interval of 6 min, we detected 7 returns. This was the highest return rate observed. Returns occurred in bursts, and one could go for several tens of minutes without getting a return and then suddenly observe a series of returns in rapid succession. This bursty character of the returns also was seen at the lunar ranging facilities.

The returns on September 28 and 29 were detected while scanning in 1-μrad increments around a 15-μrad box centered on the predicted retroreflector array coordinates. A sample of the detected returns is shown in Fig. 5. The scalar averager's detection threshold was set at $\sim$210 mV to suppress the lunar background counts. Although this limited the detection dynamic range to 5 dB (the SSPM saturated at 600-mV output in the high-gain mode), we believed that with the increased sensitivity we would increase the number of returns observed.

The scalar averager was set up at 16,000 bins, each 5.12-μs wide, for a full-screen coverage of 81.92 ms. This display setting allowed ready identification of lunar returns that were spaced 50 ms apart—the reciprocal of the laser pulse repetition rate. A 5-ms pretrigger adjustment was designed into the detection system electronics to ensure that the returns would appear away from the edge of the scalar averager's display window. Among the spurious noise spikes, Fig. 5 clearly shows lunar returns in the scalar averager's display window at 5 ms and again at 55 ms after the trigger. The 50-ms spacing corresponds to the 20-Hz laser repetition rate.

An expanded view of Fig. 5 is shown in Fig. 6. This figure clearly shows the temporal separation of the returns. Although some spurious trigger events are seen in the figure, confirmed "hits" are the spikes at 4.972, 4.977, and 54.973 ms. The small temporal dispersion in the arrival time is due to uncertainty in the trigger, which we estimate at 30 μs. The figure also shows that the returns are separated by 49.996 ms.

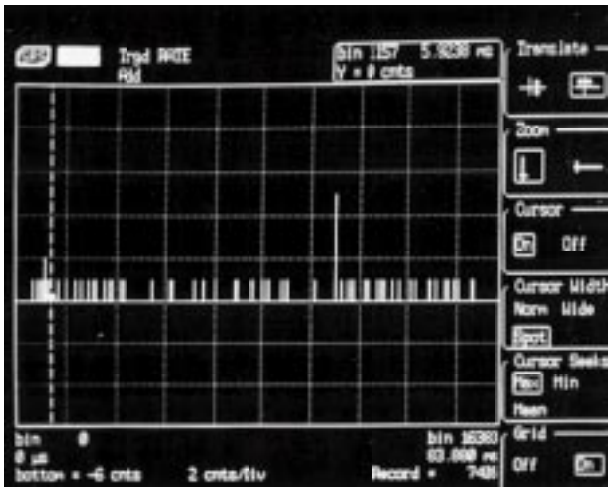

Fig. 5. Scalar average output from the September 28 transmission showing "hits" approximately 5 and 55 ms after trigger. The laser was operated at 20 Hz, and returns are approximately 50 ms apart. The window covers about 82 ms, and the vertical scale is 2 counts/division. A "hit" is any signal that exceeds the threshold of 210 mV, i.e., 27 photons.

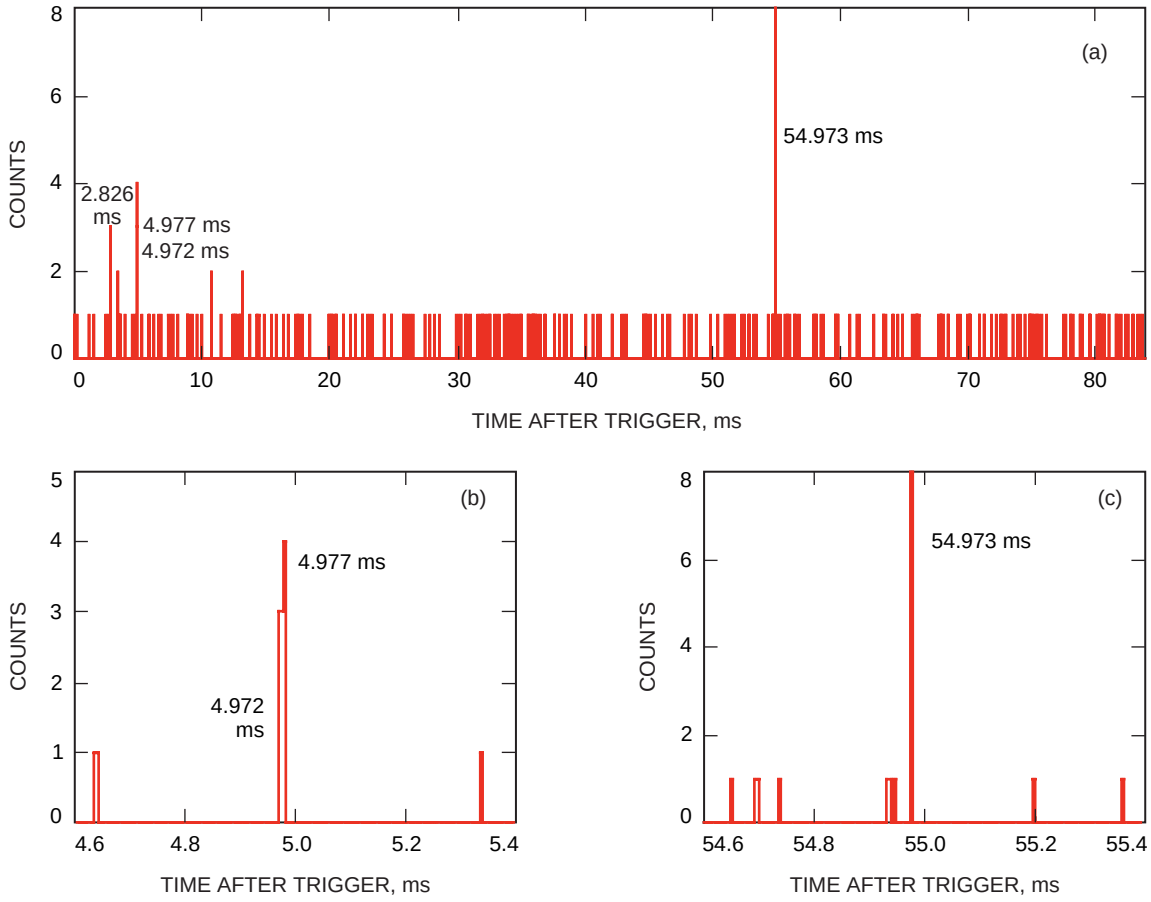

Fig. 6. An expanded view of (a) the September 28 returns shown in Fig. 5, (b) the region around 5 ms, and (c) the region around 55 ms. The window covers ~82 ms with 16-k, 5.12-μs-wide bins and shows a total of 314 counts. The spikes at 2.826 ms are outside the trigger uncertainty window and are not lunar returns.

VII. Conclusion

We successfully demonstrated the first transmission of an atmosphere-compensated laser beam to a deep-space target, the Apollo 15 retroreflectors. The transmitter was a Q-switched 340-mJ Nd:YAG laser beam with near-diffraction-limited divergence from the SOR's 1.5-m-aperture telescope. The transmitter optical train was modified to allow maximum beam throughput without introducing an arc discharge due to dust particles. The receiver was the recently built 3.5-m telescope coupled to a newly developed experimental SSPM detector at the Nasmyth focus of the telescope. The receiver was calibrated and characterized in the infrared by using stars with a high infrared signature and by Rayleigh backscatter from the 1064-nm laser beam.

Returns were detected for the compensated laser beam uplink over a 3-night period in September 1994. No returns were detected in any of the uncompensated beam propagation experiments. We think that this was because of the high threshold of our detection system. As a result, we were unable to collect sufficient data to compare experimental results with our theoretical predictions. We have identified several system-level improvements that we think would have increased both the strength and frequency of returns in future CEMERLL-type experiments. Implementing these would afford a better evaluation of the advantage of adaptive optics to deep-space optical communications. They are

(1) Use an extended-source tracker to more accurately and actively track the lunar scene and compensate for atmospheric tilt. With tilt correction implemented, we expect in excess of a 10-dB increase in signal return.

(2) Narrow the field of view of the detector and use a subnanometer bandpass filter to lower the background signal. Reducing the background will allow the detection threshold to be lowered. This would allow detection of returns from the uncompensated laser beam and afford a better comparison between the theoretical and experimental probability density functions for the signal returns.

(3) Increase the dynamic range of the detection system. The 5-dB dynamic range was the critical limitation in this experiment that precluded acquiring statistical data on the uplink beam propagation. Increasing the detector's dynamic range will be key, especially if tilt compensation is used.

Acknowledgments

The successful detection of a retroreflected uplink-compensated laser beam from the Apollo lunar retroreflectors is due to the coordination, dedication, and cooperation of several individuals. The authors would like to thank W. Rafferty and C. Edwards of JPL/Caltech for sponsoring this work through NASA's Advanced Technology Program; X. X. Newhall, also of JPL/Caltech, for providing the Chebyshev polynomials for pointing to the lunar retroreflectors; and J. R. Lesh, Supervisor of the Optical Communications Group at JPL, for his technical guidance. We thank R. Ruane for tirelessly manning the 3.5- and 1.5-m telescopes over the several months of uplink transmissions and J. Drummond for calculating the stellar intensities and identifying reference features on the Moon for offset pointing to the lunar retroreflectors. The authors extend their thanks to B. Boeke for developing the electronics and software to generate the delayed trigger to detect the return signal at the receiver, and to B. Cowan, O. Mitchell, and G. Kenyon for designing and building the beam tube that made it possible for us to gain a 30 percent increase in the transmitted power. Finally, we would like to acknowledge the support and cooperation of Col. J. Anderson, Division Head of the SOR, and that of the other members of the SOR and the Rockwell Power Systems contractor crew.

The information in this article was presented as a poster paper at the NATO Advanced Study Institute (ASI) Conference in Cargèse, France, in October 1997.

References

[1] H. Hemmati, J. Layland, J. Lesh, K. Wilson, M. Sue, D. Rascoe, F. Lansing, M. Wilhelm, L. Harcke, C. Chen, and Y. Feria, "Comparative Study of Optical and RF Communication Systems for a Mars Mission, Part II, Unified Value Metrics," *SPIE Free-Space Laser Communication Technologies Proceedings*, San Jose, California, pp. 200–214, February 1997.

[2] K. E. Wilson, J. R. Lesh, K. Araki, and Y. Arimoto, "Overview of the Ground-to-Orbit Lasercom Demonstration," Invited Paper, *SPIE Free-Space Laser Communication Technologies Proceedings*, San Jose, California, pp. 23–30, February 1997.

[3] K. E. Wilson and J. R. Lesh, "An Overview of the Galileo Optical Experiment (GOPEX)," *The Telecommunications and Data Acquisition Progress Report 42-114, April–June 1993*, Jet Propulsion Laboratory, Pasadena, California, pp. 192–204, August 15, 1993.

[4] R. Q. Fugate, "GOPEX at the Starfire Optical Range," *The Telecommunications and Data Acquisition Progress Report 42-114, April–June 1993*, Jet Propulsion Laboratory, Pasadena, California, pp. 255–279, August 15, 1993.

[5] M. Jeganathan, K. E. Wilson, and J. R. Lesh, "Preliminary Analysis of Fluctuations in Received Uplink-Beacon-Power Data Obtained from GOLD Experiments," *The Telecommunications and Data Acquisition Progress Report 42-124, October–December 1995*, Jet Propulsion Laboratory, Pasadena, California, pp. 20–32, February 15, 1996.
http://tda.jpl.nasa.gov/tda/progress_report/42-124/124J.pdf

[6] R. H. Czicky, Z. Sodnik, and B. Furch, "Design of an Optical Ground Station for In-Orbit Check-Out of Free Space Laser Communication Payloads," *SPIE Free-Space Laser Communication Technologies Proceedings*, vol. 2381, San Jose, California, pp. 26–37, February 1995.

[7] I. Kim, H. Hakakha, P. Adhikari, E. Korevaar, and A. K. Majumdar, "Scintillation Reduction Using Multiple Transmitters," *SPIE Free-Space Laser Communication Technologies IX Proceedings*, vol. 2990, San Jose, California, pp. 102–113, February 13–14, 1997.

[8] M. Jeganathan and D. Erickson, "An Overview of the Atmospheric Visibility Monitoring (AVM) Program," *SPIE Free-Space Laser Communication Technologies Proceedings*, vol. 2990, San Jose, California, pp. 14–120, February 1997.

[9] D. L. Fried, "Statistics of a Geometric Representation of Wavefront Distortion," *JOSA*, vol. 55, no. 11, pp. 1427–1435, November 1965.

[10] E. Korevaar, J. Schuster, P. Adhikari, H. Hakakha, R. Ruigrok, R. Steiger, L. Fletcher, and B. Riley, "Description of STRV-2 Lasercom Flight Hardware," *SPIE Free-Space Laser Communication Technologies IX Proceedings*, vol. 2990, San Jose, California, pp. 38–49, February 13–14, 1997.

[11] C. C. Chen and J. R. Lesh, "Applications of Laser Guide Star Technology to Deep-Space Optical Communication Systems," Laser Guide Star Workshop, Albuquerque, New Mexico, March 1992.

[12] R. Q. Fugate, B. L. Ellerbroek, C. H. Higgins, M. P. Jelonek, W. J. Lange, A. C. Slavin, W. J. Wild, D. M. Winker, J. M. Wynia et al., "Two Generations of Laser-Guide-Star Adaptive-Optics Experiments at the Starfire Optical Range," *Journal of the Optical Society of America*, vol. II, no. 1, pp. 310–324, January 1994.

[13] Lyndon B. Johnson Space Center, *Apollo 15 Preliminary Science Report*, NASA-SP-289, Houston, Texas, p. 14, 1972.

[14] P. L. Bender, D. G. Currie, S. K. Poultney, R. H. Dicke, D. H. Eckhardt, W. M. Kaula, J. D. Mulholland, H. Plotkin, E. C. Silverbery, and J. E. Faller, "The Lunar Laser Ranging Experiment," *Science*, vol. 182, pp. 229–238, October 19, 1973.

[15] Y. Arimoto, "Possibility of Very High Speed Laser Satellite Communications System Using Adaptive Optics," CRL International Symposium, Tokyo, Japan, March 12–13, 1996.

[16] K. E. Wilson, "Overview of the Compensated Earth–Moon–Earth Laser Link (CEMERLL)," *SPIE Free-Space Laser Communication Technologies Proceedings*, vol. 2123, pp. 66–74, Los Angeles, California, January 1994.

[17] M. Levine and K. Kiasaleh, "Intensity Fluctuations in the Compensated Earth–Moon–Earth Laser Link (CEMERLL) Experiment," *SPIE Free-Space Laser Communication Technologies Proceedings*, vol. 2123, Los Angeles, California, pp. 409–422, January 1994.

[18] D. Murphy, "Atmospheric-Turbulence Compensation Experiments Using Cooperative Beacons," *Massachusetts Institute of Technology Lincoln Laboratory Journal*, vol. 5, no. 1, pp. 25–44, Spring 1992.

[19] R. M. Measures, *Laser Remote Sensing*, New York: John Wiley and Sons, 1984.

[20] C. W. Allen, *Astrophysical Quantities*, London: The Athlone Press, University of London, 1983.